FINITE-MAGNETIC-REYNOLDS-NUMBER EFFECTS IN MAGNETOGASDYNAMIC FLOWS*

BY

J. Y. T. TANG AND R. SEEBASS

Cornell University

1. Introduction. Studies of magnetohydrodynamic flows with finite electrical conductivity about slender two-dimensional bodies have been carried out by many authors. These studies have included cases where the applied magnetic field is either parallel or perpendicular to the undisturbed, uniform flow field. Most of the authors, however, have confined their attention to incompressible fluid flows. For example, the incompressible analysis for the case where the magnetic field and the flow field are aligned at infinity was carried out by Lary [1]. The purpose of this investigation is to carry out the aligned-fields analysis for compressible fluids flow. These flows exhibit such interesting phenomena as forward-facing waves and up-stream wakes.

As usual, we require that the body be slender enough so that we can linearize the governing equations about a uniform state. Unfortunately, to analyze this set of equations without further simplifications would be formidable. An important simplification is to treat the case of large magnetic Reynolds number, i.e., large electrical conductivity.[1] With this assumption, a procedure using Fourier synthesis may be utilized. McCune [2] has used a similar procedure to treat the crossed-fields, incompressible case.

Our quantitative results verify the qualitative predictions of Sears and Resler [3] concerning the behavior of flows past finite bodies, based on the knowledge of the solutions for flow over infinite sinusoidal walls. Furthermore, they serve to increase our confidence in being able to observe experimentally the unusual phenomena of forward-facing waves and upstream wakes.

One begins by writing down the equations pertinent to this problem, and proceed by linearizing them about the uniform conditions at infinity. This leads to a single linear equation for the transverse component of the perturbation velocity, which in turn leads to an algebraic equation (the dispersion equation) satisfied by each of the field modes. We then write down the general form of the solution as an arbitrary combination of all these modes. With the assumption of large magnetic Reynolds number, it is possible to express the solution in a tractable form, and discuss its composition in terms of well-known phenomena. Finally, we consider a specific body shape and determine in detail the velocity and current density distributions throughout the flow.

2. Formulation. The linearized equations governing the two-dimensional motion of a compressible, electrically conducting fluid, in the presence of a magnetic field aligned with the fluid velocity far upstream of a finite disturbance, may be expressed as the single equation

---

*Received April 11, 1967.

[1]Similarly we could treat the case of small magnetic Reynolds number. However, the large magnetic Reynolds number case is more interesting because it is in this case that we have important interactions between the magnetic and flow fields.

$$\mathcal{L}\phi = \left\{(M^2 - 1)\frac{\partial^4}{\partial x^4} + (M^2 - 2)\frac{\partial^4}{\partial x^2 \partial y^2} - \frac{\partial^4}{\partial y^4} - \frac{Rm(m^2 - 1)(M^2 - 1)}{m^2}\frac{\partial}{\partial x}\left[\frac{\partial^2}{\partial x^2} - \frac{M^2 + m^2 - 1}{(M^2 - 1)(m^2 - 1)}\frac{\partial^2}{\partial y^2}\right]\right\}\phi = 0. \quad (1)$$

Here $\mathcal{L}$ is a linear, fourth-order partial differential operator, ϕ is one of the perturbations in the velocity or magnetic field components, M, m are respectively the free stream Mach and Alfvén numbers, and Rm is the magnetic Reynolds number based on a typical length. If we define the total velocity and magnetic field vectors in an (x, y)-coordinate system to be

$$\mathbf{q} = [U(1 + u), Uv], \quad \text{and} \quad \mathbf{H} = [H_\infty(1 + h_x), H_\infty h_y],$$

then all the perturbation quantities u, v, h_x , and h_y satisfy Eq. (1). This equation was first obtained by Sears and Resler [3]. We are concerned here with the structure of the solutions to this equation for large magnetic Reynolds numbers. In particular we will be concerned with the flow over a finite slender body.

When the magnetic Reynolds number is infinite, i.e., when the gas is a perfect conductor, the fourth-order differential operator degenerates to a second-order operator that is either elliptic or hyperbolic, except for certain "transition" lines, depending on the values of m and M. The graphical delineation of these regions in an (M^2, m^2)-plane, Fig. (1), has come to be known as the Taniuti-Resler-Imai diagram. Kogan [4] and Resler and McCune [5] were the first authors to give a quantitative description of the linearized flow fields associated with each of these regions. The other limit for which quantitative predictions of the behavior of the flow exist is that of incompressible flow. In this case $\mathcal{L}$ degenerates to the product of a Laplacian operator and an Oseen operator, and the solution is a linear combination of an irrotational potential flow and a parabolic wake flow. The width of the wake is proportional to $(x/Rm)^{1/2}$, and whether it is forward- or backward-facing depends on the sign of $(m^2 - 1)$. A quantitative description of the incompressible flow was first given by Lary [1].

Obviously it is not expedient to solve Eq. (1) for each of the four perturbation quantities. Because the y-component of the perturbation velocity is the quantity directly related to the body shape, we will employ Eq. (1) and the boundary condition in the body to determine this quantity. Having determined $v(x, y)$ we may use the linearized version of the continuity equation

$$(1 - M^2)\,\partial u/\partial x + \partial v/\partial y = 0 \quad (2)$$

to find $u(x, y)$. With the velocity field and hence the vorticity, $\boldsymbol{\Omega}$, prescribed we can find the electric current density, $\mathbf{J}$, by taking the curl of the linearized momentum equation with the result that

$$\mathbf{J} = m^2\boldsymbol{\Omega}. \quad (3)$$

The magnetic-field components can then be obtained from Ampère's law and the solenoidal requirement on the magnetic field, provided we assume the permeability to be constant:

$$\mathbf{J} = \nabla \times \mathbf{H}, \quad (4)$$

$$\nabla \cdot \mathbf{H} = 0. \quad (5)$$

Because we are concerned with the quantitative description of the flow past a slender obstacle, an appropriate procedure would be to formulate the boundary conditions for a finite body and obtain the solution by using Fourier transforms. Since Sears and Resler [3] have already studied some of the properties of sinusoidal solutions to Eq. (1), we can proceed to construct our solutions by means of a Fourier synthesis of these field modes. If we assume that $v(x, y)$ is proportional to $\exp(i\lambda x - ky)$, then $v(x, y)$ satisfies $\mathfrak{L}v = 0$ provided the ratio $r = k/\lambda$ satisfies the dispersion relation

$$r^2(\lambda) = 1 + \frac{M^2}{2}\left\{iK\left(\frac{M^2 + m^2 - 1}{m^2}\right) - 1 \pm \left[\left(iK\,\frac{M^2 + m^2 - 1}{m^2} - 1\right)^2 + 4iK\right]^{1/2}\right\}, \tag{6}$$

where $K = Rm/\lambda M^2$. Since the dispersion relation is biquadratic, there are four values of r for which $\mathfrak{L}v = 0$. Two of these will lead to v's that vanish as $y \to \infty$, while their conjugates will give v's that are unbounded as $y \to \infty$. Keeping only the two values of r that lead to bounded solutions, we may express v as

$$v(\lambda; x, y) = V_1(\lambda) \exp[\lambda(ix - r_1 y)] + V_2(\lambda) \exp[\lambda(ix - r_2 y)],$$

where the arbitrary functions of λ are to be determined from the boundary conditions.

We are interested in predicting quantitative features of the flow field about a finite slender body. In particular, we wish to examine the flow field itself, rather than the forces on the body, because it is important to predict those magneto-aerodynamic features that may be observed in laboratory experiments. For this reason, and mathematical simplicity as well, we limit our attention to symmetric bodies. For a finite body the solution $v(x, y)$ must consist of contributions from all wave numbers, λ. Thus the general solution for a finite body has the form

$$v(x, y) = \int_{-\infty}^{\infty} [V_1(\lambda) \exp(-r_1\lambda y) + V_2(\lambda) \exp(-r_2\lambda y)] \exp(i\lambda x)\, d\lambda. \tag{7}$$

Here we have included negative λ's as well, simply for mathematical convenience. With our body shape prescribed and symmetrical about the x-axis, the inviscid boundary condition on the velocity prescribes the distribution of v on the surface of the body. Under the mean-surface approximation this reduces to prescribing $v(x, 0)$ on the x-axis. Thus

$$V_1(\lambda) + V_2(\lambda) = \frac{1}{2\pi}\int_{-\infty}^{\infty} v(s, 0) \exp(-i\lambda s)\, ds. \tag{8}$$

Another relation between the V's must be supplied by an additional boundary condition. Besides the usual inviscid fluid dynamic boundary conditions, we have boundary conditions on the electromagnetic quantities. Because there is no applied electric field when the velocity and magnetic field vectors are aligned at infinity, the latter are simply that the magnetic induction be continuous through the surface. We shall take the permeability of the body to be the same as that of the fluid, and impose this continuity on the magnetic field vector **H**. This boundary condition, coupled with the requirement that both components of **H** be harmonic inside the body, leads to another linear relationship between V_1 and V_2. For a slender body this reduces to the requirement that $h_y(x, 0)$ vanish and yields, with the aid of Eqs. (2)–(5),

$$V_2(\lambda) = -Q(\lambda) V_1(\lambda), \tag{9}$$

where

$$Q(\lambda) = \frac{(r_2^2 - 1)(1 - M^2 - r_1^2)}{(r_1^2 - 1)(1 - M^2 - r_2^2)}.$$

The subscripts 1, 2 refer to the +, − signs in Eq. (6). Combining Eqs. (8) and (9) we find

$$V_1(\lambda) = \frac{1}{2\pi}[1 - Q(\lambda)]^{-1} \int_{-\infty}^{\infty} v(s, 0) \exp(-i\lambda s)\, ds. \tag{10}$$

With $V_1(\lambda)$ and $V_2(\lambda)$ determined, we may then use Eqs. (2)–(5) to express each of the perturbations in terms of $V_1(\lambda)$ and $V_2(\lambda)$:

$$\begin{aligned}
i(1 - M^2)u(x, y) &= \int_{-\infty}^{\infty} \{r_1(\lambda) V_1(\lambda) \exp[-\lambda r_1(\lambda) y] \\
&\qquad + r_2(\lambda) V_2(\lambda) \exp[-\lambda r_2(\lambda) y]\} \exp(i\lambda x)\, d\lambda, \\
v(x, y) &= \int_{-\infty}^{\infty} \{V_1(\lambda) \exp[-\lambda r_1(\lambda) y] \\
&\qquad + V_2(\lambda) \exp[-\lambda r_2(\lambda) y]\} \exp(i\lambda x)\, d\lambda, \\
im^{-2}(M^2 - 1)h_x(x, y) &= \int_{-\infty}^{\infty} \left\{ \frac{r_1(\lambda)[1 - M^2 - r_1^2(\lambda)]}{r_1^2(\lambda) - 1} V_1(\lambda) \exp[-\lambda r_1(\lambda) y] \right. \\
&\qquad \left. + \frac{r_2(\lambda)[1 - M^2 - r_2^2(\lambda)]}{r_2^2(\lambda) - 1} V_2(\lambda) \exp[-\lambda r_2(\lambda) y] \right\} \exp(i\lambda x)\, d\lambda, \\
m^{-2}(M^2 - 1)h_y(x, y) &= \int_{-\infty}^{\infty} \frac{1 - M^2 - r_1^2(\lambda)}{r_1^2(\lambda) - 1} V_1(\lambda) \exp[-\lambda r_1(\lambda) y] \\
&\qquad + \frac{1 - M^2 - r_2^2(\lambda)}{r_2^2(\lambda) - 1} V_2(\lambda) \exp[-\lambda r_2(\lambda) y] \exp(i\lambda x)\, d\lambda.
\end{aligned} \tag{11}$$

Because the highest-order terms in the operator $\mathfrak{L}$ can be written as the product of a Laplacian and a Prandtl-Glauert operator, it is necessary to specify either one or two cylcic constants, depending on the Mach number. The additional cyclic constant that arises here is determined by specifying the total current inside the body. However, for a symmetric body with no current flowing inside, both the cyclic constants are zero.

Equations (9), (10), and (11) complete our description of linearized magnetogasdynamic flow past a slender body. Of course, there remains the important question of when our linearization is applicable. If we let ϵ be representative of the body slope, then it is possible to show that outside the magnetogasdynamic boundary layer and wake,[2] all the perturbations are at most $O(\epsilon)$. Inside the boundary layer, however, such a conclusion is not possible. The linearized version of Ohm's law requires that $J = Rm(h_y - v)$ and our boundary conditions then demand $J = O(Rm\epsilon)$ near the body.

[2]The terms "boundary layer" or "wake" which we have used here describe phenomena that are merely diffuse Alfvén waves. But in the case of aligned-fields flow, these waves are nearly, to $O(\epsilon)$, parallel or anti-parallel to the free stream. Having originated from either the leading or the trailing edge of the disturbance and having the usual parabolic structure in the normal direction, they will be described here as boundary layers or wakes.

With current densities of this magnitude, the body force term in the momentum equation is $O(S\epsilon)$, where $S = m^{-2}Rm$ is the usual interaction parameter. Thus we cannot expect the perturbations to remain $O(\epsilon)$ near the body. A careful analysis of the order of magnitude of the terms in this boundary layer (see Sears [6]) shows that the largest perturbations are $O(S^{1/2}\epsilon)$. Consequently we must require $S^{1/2}\epsilon = o(1)$ for our linearization to be valid. Because the Joule dissipation is $O(S\epsilon^2)$, it may always be neglected if the perturbations themselves are small.

3. Large magnetic Reynolds number. The solution to the problem we have formulated in the previous section may be represented formally by combining Eqs. (9)–(11). For example, the transverse velocity perturbation in the upper-half plane is given by

$$v(x, y) = \frac{1}{2\pi}\int_{-\infty}^{\infty}\int_{-\infty}^{\infty} v(s, 0)[1 - Q(\lambda)]^{-1} \exp\{i\lambda[x - s + ir_1(\lambda)y]\}\, d\lambda\, ds - \frac{1}{2\pi}\int_{-\infty}^{\infty}\int_{-\infty}^{\infty} v(s, 0)Q(\lambda)[1 - Q(\lambda)]^{-1} \exp\{i\lambda[x - s + ir_2(\lambda)y]\}\, d\lambda\, ds. \tag{12}$$

Even for the simplest choices of $v(s, 0)$, the complicated functional dependence of the roots of the dispersion relation on λ makes the evaluation of these integrals formidable, if not impossible. To obtain an analytic description of the flow field it is necessary for us to approximate the integrands in Eq. (12). In this regard the quantity of primary importance in the dispersion relation is $K = Rm/\lambda M^2$. For small values of this parameter the magnetogasdynamic effects will be perturbations on the ordinary gasdynamic flow field. On the other hand, for large values of K we expect all the new and interesting magnetogasdynamic phenomena to be present. Although present day experiments of the flow past bodies seem to be confined to low and possibly moderate values of K, it is anticipated that in the near future experiments for compressible media will be extended to reasonably large values of K. With this possibility in mind, and because we are interested in exploring the nature of the flow field in different regions of the Taniuti-Resler-Imai diagram, we shall limit our investigation to the case of large magnetic Reynolds number, i.e., to large K.

From the nature of the roots of the dispersion relation, we can see that periodic solutions consist of damped waves, and that the damping, and in some cases the wave angle, is dependent upon the wavelength of excitation. This behavior is simplified when we consider the asymptotic form of the roots for large K:

$$\begin{aligned} r_1 &= \pm c^{-1}M^2(Rm/2\lambda M^2)^{1/2}(1 + i) + O(K^{-1/2}), \\ r_2 &= \pm(c^2 - 1)^{1/2}[i - \lambda c^4/2Rm(1 - m^2)] + O(K^{-2}). \end{aligned} \tag{13}$$

Here we have introduced the parameter $c^2 = m^2M^2/(m^2 + M^2 - 1)$; the transitions from elliptic to hyperbolic behavior in Fig. (1) occur at $m = 1$, $M = 1$, and $c^{-1} = 0$. In Eqs. (13) the plus or minus sign must be chosen for r_1 when $c^{-2} > 0$ or $c^{-2} < 0$ to insure that the disturbances vanish at infinity. For the same reason the following signs must be chosen for r_2 : the plus sign for $c^{-2} < 0$; the plus or minus sign for $m^2 > 1$ or $m^2 < 1$ when $c^2 > 1$; the minus sign for $c^{-2} > 1$.

Under the hypothesis of large magnetic Reynolds number, we see that the first root (13) corresponds to an exponential damping of the disturbance proportional to $yRm^{1/2}$. Thus the disturbance is confined to a wake-like region about the x-axis. In contrast, for $c > 1$, the damping of the second root is proportional to yRm^{-1}. Further-

more the inclination of the lines of constant phase corresponding to this root is independent of λ. Thus the structure of this contribution is wave-like. On the other hand, when $c^2 < 1$, the damping of the second root is proportional to y and the inclination of lines of constant phase is dependent on λ. This behavior is typical of solutions to elliptic equations. The complete solution for large magnetic Reynolds number consists of the superposition of a parabolic and either a hyperbolic or an elliptic behavior.

With the simplifications afforded by (13) and the expansion

$$Q(\lambda) = m^2/(1 - M^2) + O(\lambda/Rm)$$

we may rewrite Eq. (12) for large K

$$v(x, y) = \frac{M^2 - 1}{2\pi(m^2 + M^2 - 1)} \int_{-\infty}^{\infty} \int_{-\infty}^{\infty} v(s, 0) \exp \{i\lambda[x - s \mp |c^{-1}| M(Rm/2 |\lambda|)^{1/2} y] - |c^{-1}| M(Rm/2 |\lambda|)^{1/2} |\lambda| y\} \, ds \, d\lambda \quad \mp \text{ for } C^{-2} \gtrless 0 \tag{14}$$

$$+ \frac{m^2}{2\pi(m^2 + M^2 - 1)} \int_{-\infty}^{\infty} \int_{-\infty}^{\infty} v(s, 0) \exp \{i\lambda[x - s \mp (c^2 - 1)^{1/2} y] \pm \sigma\lambda^2 y\} \, ds \, d\lambda, \quad \text{for } c^2 \gtrless 1$$

where we have introduced the parameter $\sigma = (c^2 - 1)^{1/2} c^4/2Rm(1 - m^2)$ to simplify the second integrand. The first term on the right-hand side represents the parabolic contribution to the solution and the second term the contribution that corresponds to either elliptic or hyperbolic behavior.

We know that for large K the integrands in (14) are valid replacements for the integrands in (12). This does not necessarily mean, however, that (14) is a suitable representation for $v(x, y)$. The parameter K is large when Rm/M^2 is large provided that λ takes on small or moderate values; for large values of λ, K will be moderate or small. Because the integrations in Eqs. (12) and (14) are carried out over all λ, we must also consider the contributions that arise for large λ, i.e., moderate or small values of K. Thus, to show that (14) is a valid representation of the solution, it is necessary to show that for large λ both the spurious contribution to (14) and the true contribution to (12) are negligible. For $(Rmy)^{-1} = o(1)$ one may easily show that the difference between our approximate solution and the true solution is $O[Rmy/(1 + x^2)^{1/2}]$. On the other hand, for $Rmy = O(1)$ the above requirement is too stringent; it is only necessary that for large λ the difference between the spurious contribution and the true contribution be small. In this case we may show the error to be $O[Rmy/(1 + x^2)^{1/2}]$ compared to 1. Thus for large and small values of Rmy, the representation (14) is a valid approximation to (12) for large Rm. We hypothesize that (14) is indeed a valid replacement for (12) for all Rmy and x, with the possible exception of a circular regions of diameter $O(Rm^{-1})$ centered at the leading and trailing edges. A more detailed investigation (Tang [7]) of the expressions (12) and (14), and the behavior of our results for $Rmy = O(1)$ support this hypothesis. However, short of carrying out the integration over λ for Eq. (12), it is impossible to prove this hypothesis for $Rmy = O(1)$. Furthermore, our analytical results suggest that in the leading- and trailing-edge regions excepted above the error in (14) relative to (12) may be $O(1)$.

Because we are considering a finite body of length L, and the coordinates have been nondimensionalized by this length, the s-integration in Eq. (14) need only be con-

sidered over the range $[-\frac{1}{2}, \frac{1}{2}]$. Outside of this interval $v(s, 0)$ is zero for a symmetric body. We can carry out the integration over λ now that the integrands' dependence on λ has been simplified. With this end in mind, we rewrite (14) as

$$v(x, y) = \frac{1}{2\pi(m^2 + M^2 - 1)} \int_{-1/2}^{1/2} v(s, 0)[(M^2 - 1)I_1(s) + m^2 I_2(s)]\, ds, \tag{15}$$

where

$$I_1(s) = \int_{-\infty}^{\infty} \exp\{i\lambda[x - s \mp c^{-1}M(Rm/2\,|\lambda|)^{1/2}y] \mp c^{-1}M(Rm\,|\lambda|/2)^{1/2}y\}\, d\lambda,$$

and

$$I_2(s) = \int_{-\infty}^{\infty} \exp\{i\lambda[x - s \mp (c^2 - 1)^{1/2}y] \pm \sigma\lambda^2 y\}\, d\lambda.$$

The integrals I_1 and I_2 correspond to the parabolic and elliptic or hyperbolic contributions to the solution.

We begin by investigating the simpler of the two integrals (15), I_1 . Clearly this integral represents a superposition of highly damped waves that are inclined either backward or forward when $c^{-2} > 0$ or $c^{-2} < 0$. If we consider λ as a complex variable, then the appropriate branch cut to render the integrand single-valued is along the positive imaginary axis of the λ-plane for $c^{-2} > 0$ and along the negative imaginary axis for $c^{-2} < 0$. To evaluate I_1 we consider the following contour integral: The real axis with a suitable indentation about the branch point, the semicircle at infinity in the upper half-plane for $c^{-2}(x - s) > 0$, or the semicircle at infinity in the lower half-plane for $c^{-2}(x - s) < 0$. When the semicircle is in the half-plane of the branch cut the contour is to be deformed about the cut. Since there are no poles in the integrand and the contributions from the semicircle vanish, the only instances when I_1 is not identically zero are when the branch cut is in the half-plane where the integrand vanishes at infinity. Thus the only contribution comes from integrating along the branch cuts, i.e., along the positive or negative imaginary axis. On these axes the integrand is purely real and its integral is the form of a tabulated Laplace transform. The final result is simply

$$I_1 = \begin{cases} M\,|c^{-1}|\,(\pi Rm)^{1/2}y\,|x - s|^{-3/2} \exp[-M^2\,|c^{-2}|\,y^2 Rm/4\,|x - s|]; & c^{-2}(x - s) > 0 \\ 0; & c^{-2}(x - s) < 0 \end{cases}. \tag{16}$$

To investigate the second of the two integrals, it is necessary to consider separately the hyperbolic case ($c^2 > 1$) and the elliptic case ($c^2 < 1$). For the first case, which we will designate by I_H, we have

$$\begin{aligned} I_H &= \int_{-\infty}^{\infty} \exp\{i\lambda[x - s \mp (c^2 - 1)^{1/2}y] \pm \sigma\lambda^2 y\}\, d\lambda \\ &= \left(\frac{\pi}{|\sigma|\, y}\right)^{1/2} \exp\{-[x - s \mp (c^2 - 1)^{1/2}y]/4\,|\sigma|\, y\}; \qquad m^2 \gtrless 1. \end{aligned} \tag{17}$$

This integral represents the wave contributions in the hyperbolic regions of Fig. (1).

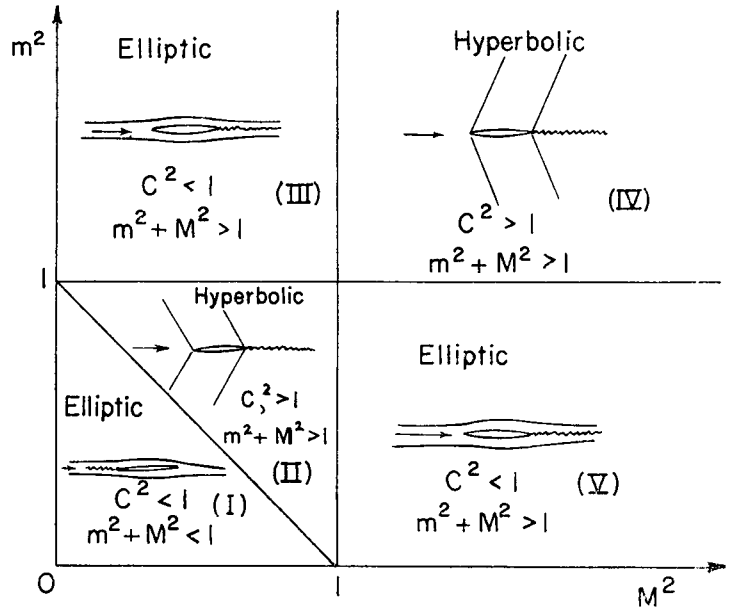

FIG. 1. The Taniuti-Resler-Imai (TRI) diagram.

The cotangent of the angle at which the wave is inclined to the y-axis is $(c^2 - 1)^{1/2}$ sgn $(m^2 - 1)$; for $m^2 > 1$ or $m^2 < 1$ the wave is inclined backward or forward with respect to the free stream. Note that the contribution of I_H to the solution is negligible outside the region where $[x - s \mp (c^2 - 1)^{1/2}y] \leq O(Rm^{-1})$; the wave structure is diffused throughout this region which is essentially a parabola centered on a line drawn at the wave angle for $Rm^{-1} = 0$.

For $c^2 < 1$, the integral I_2 represents an elliptic flow field. Note that here σ is imaginary. This integral contributes lightly damped waves that have their angle of inclination with the y-axis proportional to λ. For our purposes, the most convenient representation is

$$I_E = 2\int_0^\infty \cos[\lambda(x - s - \sigma y\lambda)] \exp[-(1 - c^2)^{1/2}\lambda y]\, d\lambda$$
$$= \Re\left\{\left(\frac{\pi}{|\sigma|\, y}\right)^{1/2} \exp(\pm i\pi/4) W\left(\frac{-\exp(\mp i3\pi/4)}{2(|\sigma|\, y)^{1/2}}[x - s + i(1 - c^2)^{1/2}y]\right)\right\}, \quad m^2 \gtrless 1. \tag{18}$$

Here $W(z)$ is defined by

$$W(z) = \exp(-z^2)\, \mathrm{erfc}\,(-iz)$$

and $\Re(z)$ indicates the real part of z. When $[x - s - i(1 - c^2)y] = O(1)$ the argument of the W-function is $O(Rm^{1/2}y^{-1/2})$. For large values of the argument we may use the asymptotic form of W to conclude $I_E = O(1)$. For small values of the argument, i.e., for $(Rm/y)^{1/2} = o(1)$, $I_E = O(Rm^{1/2}y^{-1/2}) = o(1)$, and its contribution to the solution is negligible. A more detailed examination of (18) shows that even when $(x - s)$ and y both approach zero, the asymptotic expansion is sufficient to provide the correct limiting value as $y \to 0$. Thus, if we replace Eq. (18) by its asymptotic expansion,

$$I_E = \frac{2(1-c^2)^{1/2}y}{(x-s)^2+(1-c^2)y^2}\left[1+O\left\{\frac{(x-s)yRm^{-1}}{[(x-s)^2+(1-c^2)y^2]^2}\right\}\right]; \tag{19}$$

then we introduce an error that is $O(Rm^{-1})$ relative to the leading term.

Finally, we can express $v(x, y)$ as the sum of a parabolic contribution, $v_p(x, y)$, and either a hyperbolic contribution $v_H(x, y)$, or an elliptic contribution $v_E(x, y)$:

$$v_p(x,y) = \left\{\begin{array}{ll} 0, & x < -\frac{1}{2} \\ \dfrac{(M^2-1)c}{2Mm^2}\left(\dfrac{Rm}{\pi}\right)^{1/2} y \displaystyle\int_{-1/2}^{\min(x,1/2)} v(s,0)\,\frac{\exp\,[-(c^{-1}My)^2Rm/2(x-s)]}{(x-s)^{3/2}}\,ds, & x > -\frac{1}{2} \end{array}\right\} \quad \text{for } c^{-2} > 0; \tag{20}$$

$$v_p(x,y) = \left\{\begin{array}{ll} -\dfrac{(M^2-1)\,|c|}{2Mm^2}\left(\dfrac{Rm}{\pi}\right)^{1/2} y \displaystyle\int_{\max(x,-1/2)}^{1/2} v(s,0)\,\frac{\exp\,[(c^{-1}My)^2Rm/2(s-x)]}{(s-x)^{3/2}}\,ds, & x < \frac{1}{2} \\ 0, & x > \frac{1}{2} \end{array}\right\} \quad \text{for } c^{-2} < 0;$$

$$v_H(x,y) = \frac{c^2}{2\pi M^2}\left(\frac{\pi}{|\sigma|\,y}\right)^{1/2}\int_{-1/2}^{1/2} v(s,0)\,\exp\,\{-[x-s\mp(c^2-1)^{1/2}y]^2/4\,|\sigma|\,y\}\,ds; \quad m^2 \gtrless 1; \tag{21}$$

$$v_E(x,y) = \frac{c^2(1-c^2)^{1/2}y}{\pi M^2}\int_{-1/2}^{1/2}\frac{v(s,0)}{(x-s)^2+(1-c^2)y^2}\,ds; \tag{22}$$

$$v(x,y) = v_p(x,y) + \left\{\begin{array}{l} v_H(x,y) \\ v_E(x,y) \end{array}\right\}.$$

4. Example and results. The formulae (19) through (22) constitute the approximate solution for large magnetic Reynolds number to Eq. (1) with $v(x, 0) = 0$ for $|x| > \frac{1}{2}$, $v(x, 0)$ prescribed by the body shape for $|x| \leq \frac{1}{2}$, and $v(x, y) \to 0$ as $x^2 + y^2 \to \infty$. The first of these expressions (19) exhibits wake-like behavior: lines of constant damping are asymptotic to the parabola $Rmy^2 = x$, and there is an algebraic decay proportional to $x^{-3/2}$. This wake develops behind the body for $c^{-2} > 0$ and in front of the body for $c^{-2} < 0$. The second expression (21) embodies lightly damped waves about the lines $x \pm \frac{1}{2} = \mp(c^2 - 1)^{1/2}y$; for $m^2 < 1$ the waves are forward-facing and for $m^2 > 1$ they are rearward-facing. The elliptic nature of the third result (22) is manifest in the integrand: the kernel of the integrand is simply the Green's function for a Prandtl-Glauert operator.

To proceed we need only to specify the body shape. Our choice should be a function that makes the integrals tractable; it should also have discontinuities at the leading and trailing edges so that the waves that occur in the hyperbolic regions originate as discontinuities. Within these limitations an appropriate choice is the biconvex profile whose upper surface is given by $y(x) = \epsilon \cos \pi x$, and thus $v(x, 0) = -\pi\epsilon \sin \pi x$; $|x| \leq \frac{1}{2}$.

We begin with the parabolic portion of the solution. Replacing the variable of integration by $(x - s)^{-1/2}$, we recognize the resulting integral as an error function, which

we represent in terms of the W-function as

$$v_p(x, y) = \begin{cases} 0 & , \text{ for } (\operatorname{sgn} c^{-2})x < -\tfrac{1}{2} \\ B(x + \tfrac{1}{2}, y) & , \text{ for } |x| \leq \tfrac{1}{2} \\ B(x + \tfrac{1}{2}, y) + B(x - \tfrac{1}{2}, y), & \text{for } (\operatorname{sgn} c^{-2})x > \tfrac{1}{2} \end{cases}, \tag{23}$$

where

$$B(x \pm \tfrac{1}{2}, y) = \frac{\pi\epsilon c^2(M^2 - 1)}{2m^2M^2} \exp \frac{1}{4}\left[\frac{-RmM^2\,|c^{-2}|\,y^2}{(\operatorname{sgn} c^{-2})x \pm \frac{1}{2}}\right]$$
$$\cdot \Re\left\{W\left(\left\{\frac{\pi}{2}\left[(\operatorname{sgn} c^{-2})x \pm \tfrac{1}{2}\right]\right\}^{1/2}(1 + i) + \frac{iMRm^{1/2}y}{2\,|c|\,[(\operatorname{sgn} c^{-2})x \pm \frac{1}{2}]^{1/2}}\right)\right.$$
$$\left. + W\left(-\left\{\frac{\pi}{2}\left[(\operatorname{sgn} c^{-2})x \pm \tfrac{1}{2}\right]\right\}^{1/2}(1 + i) + \frac{iMRm^{1/2}y}{2\,|c|\,[(\operatorname{sgn} c^{-2})x \pm \frac{1}{2}]^{1/2}}\right)\right\}.$$

Thus we see that the effect of finite electrical conductivity has introduced a wake in place of the current sheets that envelop the body when the electrical conductivity is infinite. For large x, i.e., $x = O(Rm)$, the W-functions are asymptotic to $x^{-1/2}$ and the thickness of the wake is $O(x/Rm)^{1/2}$. In this wake the horizontal velocity component, which may be deduced from Eq. (2), is $O(\epsilon Rm^{1/2})$. Consequently we must require $\epsilon Rm^{1/2} = o(1)$ for our linearization to be valid in the magnetogasdynamic boundary layer and wake.

For the hyperbolic contribution to the solution, the integral (21) can also be recognized as an error function by completing the square of variable of integration. The result is

$$v_H(x, y) = \operatorname{sgn}(1 - m^2)\,\frac{\pi\epsilon c^2}{2M^2} \exp(-\pi^2\,|\sigma|\,y)$$
$$\cdot g\{\exp[-i\pi x \operatorname{sgn}(1 - m^2) - i\pi(c^2 - 1)^{1/2}y][\operatorname{erf} H_+(x, y) + \operatorname{erf} H_-(x, y)]\}. \tag{24}$$

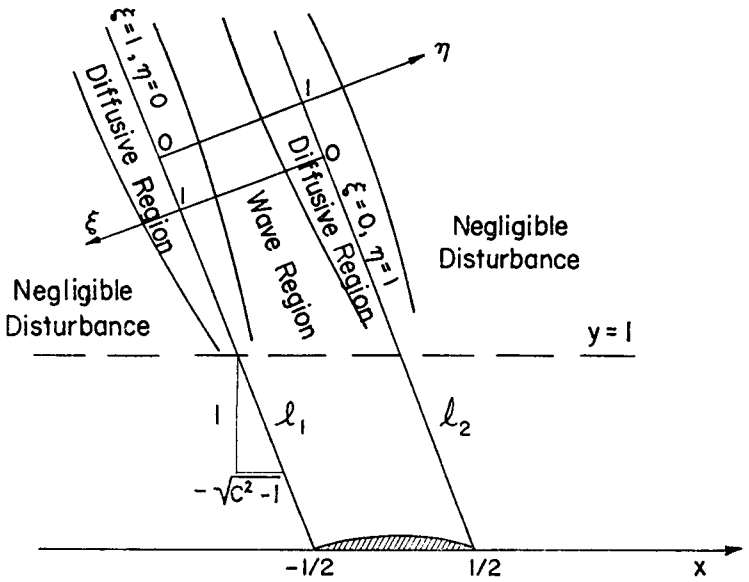

FIG. 2. Coordinate system for description of the wave component of the solution.

Here

$$H_{\pm}(x, y) = \frac{\frac{1}{2} \pm x \operatorname{sgn}(1 - m^2) \pm (c^2 - 1)^{1/2} y}{2(|\sigma|\, y)^{1/2}} \mp i\pi(|\sigma|\, y)^{1/2}$$

and $\Im(z)$ denotes the imaginary part of z. The interpretation of (24) is facilitated by introducing the coordinates ξ, $\eta = \frac{1}{2} \pm x \operatorname{sgn}(1 - m^2) \pm (c^2 - 1)^{1/2} y$. These coordinates designate the distances normal to the infinite conductivity wave fronts l_1 and l_2 as sketched in Fig. (2). With Eq. (24) rewritten in terms of these coordinates it it easy to see that there are two diffuse regions where the disturbances are not negligible. In these regions the magnitudes of the disturbances are damped to e^{-1} of their values on l_1 or l_2 in a distance of $|\xi|$ or $|\eta| = O((x/Rm)^{1/2})$ for $y = O(1)$. The effect of finite electrical conductivity is to allow diffusion to occur about the position of the infinite Rm standing wave pattern. The structure of these diffuse regions is parabolic in y as we anticipated.

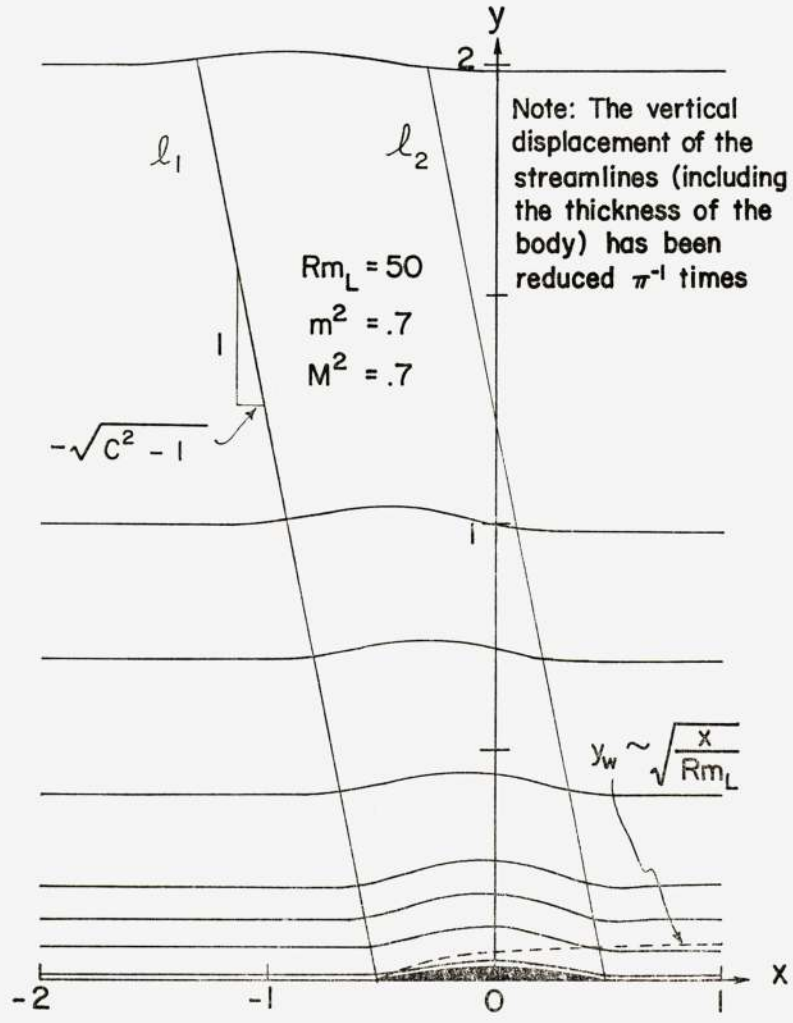

FIG. 3. Flow field in region II of TRI diagram for the biconvex profile.

Finally, by making a suitable change of variables, the elliptic contribution of our solution can be expressed in terms of the exponential integral, E_1, as follows:

$$V_E(x, y) = \frac{\epsilon c^2}{2M^2} \Re\{e^{-i\pi z}[E_+(x, y) \exp(-\pi(1 - c^2)^{1/2}y) - E_-(x, y) \exp(\pi(1 - c^2)^{1/2}y)]\},$$

where

$$E_\pm(x, y) = E_1[\mp\pi(1 - c^2)^{1/2}y - i\pi(x + \tfrac{1}{2})] - E_1[\mp\pi(1 - c^2)^{1/2}y - i\pi(x - \tfrac{1}{2})] - (1 \pm 1)\frac{\pi i}{2}[1 - \operatorname{sgn}(|x| - \tfrac{1}{2})]. \quad (25)$$

The behavior of solutions of this type is well known but difficult to describe. We shall not attempt to elaborate on its various features here, except to note that the discontinuity in E_1 provides the discontinuity in $v(x, 0)$ at the leading and trailing edges of the body.

In any magnetogasdynamic problem it is essential that we fully understand the role of the Lorentz force in influencing the flow field. To do so, we must first determine the distributions of the current density, $J(x, y)$. This is carried out by following the procedure outlined in the Formulation. The resultant expressions for the current density

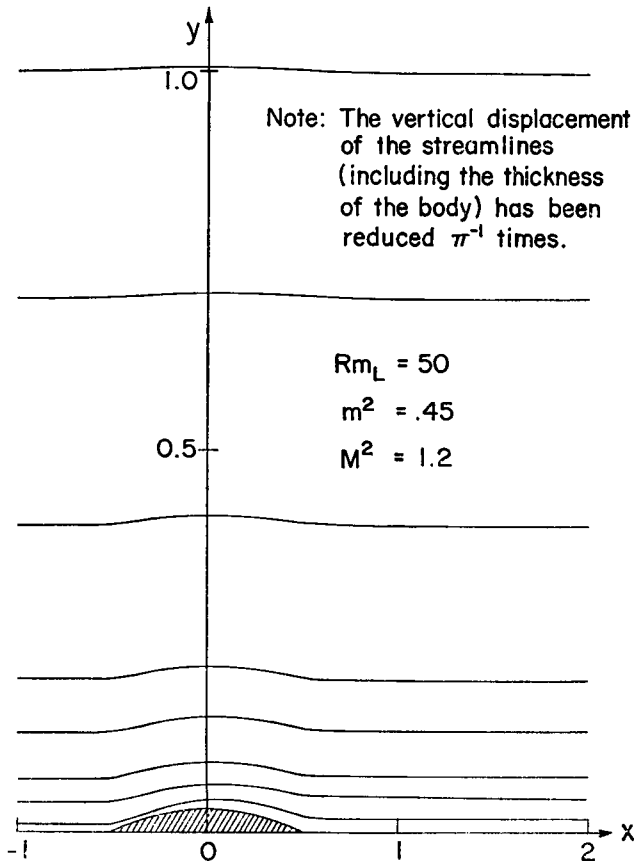

FIG. 4. Flow field in region V of TRI diagram for the biconvex profile.

may be found in Tang [7]. Because these analytical descriptions add little qualitative insight for describing the flow fields and the current density distributions, we shall employ graphical representation of these solutions in different regions of the Taniuti-Resler-Imai diagram. To avoid needless repetitions, only the solutions of regions II and V are included. Fig. (3) displays the flow field of a forward-facing wave and a backward wake; Fig. (4) exhibits that of an elliptic behavior and a backward wake. These figures are self-explanatory and need no elaboration. Corresponding plots of current density distributions are given in Figs. (5) and (6).

The plots of the current density distributions reveal many interesting phenomena For example, the elliptic component is symmetric about the y-axis and its magnitude is negligible in comparison with that of the wake component. The finiteness of this component is the result of the compressibility of our gas, and J_E vanishes as the Mach number approaches zero. For $M = 0$ we recover the irrotational incompressible solution of Lary [1]. The asymptotic behavior of the current density associated with the wake component has the general character of a boundary-layer solution. Its algebraic decay in x is $x^{-5/2}$. This does not appear to agree with the decay of $x^{-3/2}$ predicted by Fan [8] for a body of general shape. A study of the discrepancy reveals, however, that this is entirely due to the fore-and-aft symmetry of the body we have chosen and which annihilates the coefficient of the $x^{-3/2}$ term. Lastly, the plot of current density distribution associated with the wave component displays the parabolic growth of the diffusive regions with increasing y as expected.

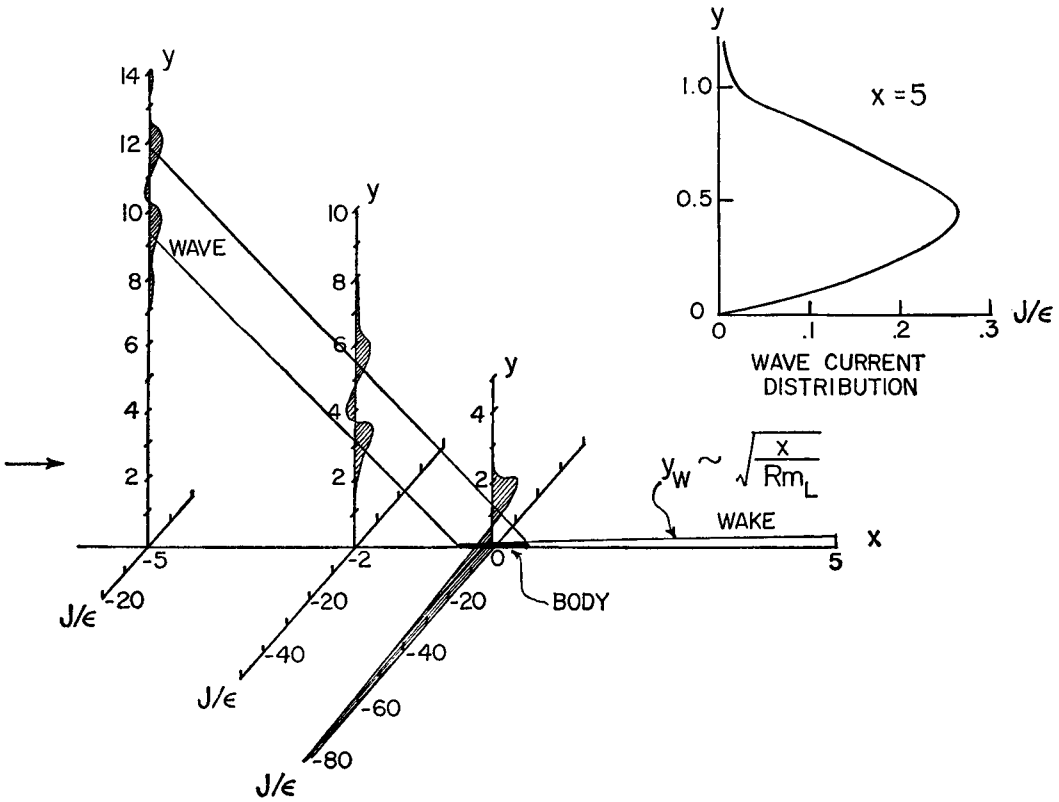

FIG. 5. Distribution of current density in region II of TRI diagram for the biconvex profile.

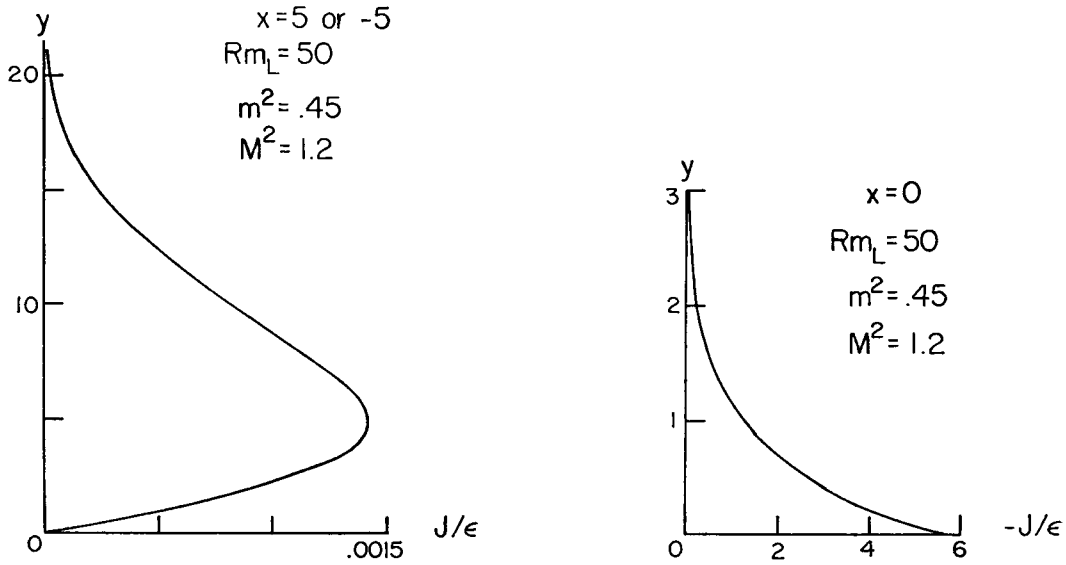

FIG. 6. Distribution of the elliptic component of the current density for the biconvex profile.

The behavior of J for large y indicated by Fig. (5) is interesting. Oscillations, which are absent at smaller values of y, appear in the diffusive regions about the wave fronts. Because these oscillations disappear when we increase Rm with y fixed, one might attribute them to the cut-off error introduced by our approximate Fourier synthesis. However, our analysis of the cut-off error seems to negate this possibility. To clarify this situation, we considered the problem of flow past a ramp body having the same initial flow deflection angle as our biconvex profile [see Fig. (7)]. A comparison of the transverse velocity component[3] for the ramp body and for the biconvex profile is made in Fig. (8). From this figure we conclude that the additional oscillations noticed at large y in Fig. (5) result from the varying slope of our body rather than from cut-off errors introduced by the finite flow deflection angle at the leading and trailing edges. Referring back to Eq. (21), we can explain this conclusion as follows: because σy varies like y/Rm, the exponential part of the integrand serves to filter out a narrow or broad portion of the slope of the body depending on whether $y = O(Rm)$ or $y \ll Rm$, the former being

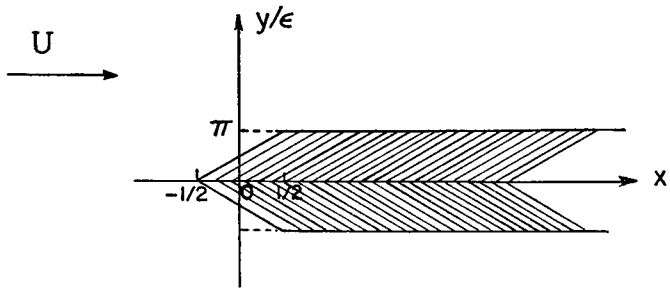

FIG. 7. The ramp body.

[3]By virture of the linearized Ohm's law and the linear relationship between v and h_y this procedure is equivalent to a comparison of the current densities.

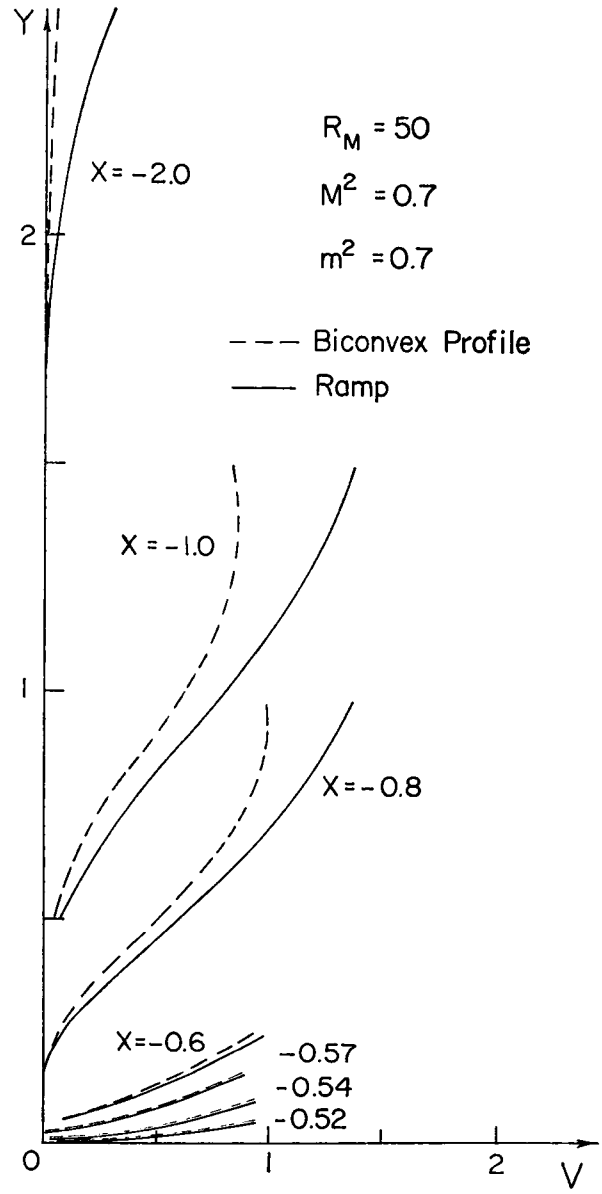

FIG. 8. Comparison of the hyperbolic component of the transverse velocity, v_H, near the leading edges of a ramp and a biconvex profile.

the case where the oscillations occur. The exponential part of the integrand picks up more and more of the negative portion of the sinusoid as we move inward from the outer edge of the diffusive region. This cancels the contribution from the positive portion of the sinusoid and produces the oscillations.

5. Conclusion. We have succeeded in quantitatively determining the effects of large but finite *Rm* upon aligned-fields magnetogasdynamic flow. Analytical solutions for both the flow fields and the current density distributions in all regions of the Taniuti-

Resler-Imai diagram have been obtained and plotted with the results showing remarkable consistency with the assumptions of this analysis. Our small-perturbation solutions exist everywhere provided $(Rm)^{1/2}\epsilon = o(1)$, are valid when $Rm^{-1} = o(1)$ and satisfy the appropriate boundary conditions on the body and at infinity.

Acknowledgment. The authors are indebted to Professor Isao Imai, Professor E. L. Resler, Jr. and Dr. D. N. Fan for their helpful discussions of many aspects of this investigation. This study was supported by the U.S. Air Force Office of Scientific Research under contract AF 49(638)-1346.

References

1. E. C. Lary, *A theory of thin airfoils and slender bodies in fluids of finite electrical conductivity with aligned-fields*, Jr. of Fluid Mech. **12**, 209 (1962)
2. J. E. McCune, *On the motion of thin airfoils in fluids of finite electrical conductivity*, Jr. of Fluid Mech. **7**, 449 (1960)
3. W. R. Sears and E. L. Resler, Jr., *Magneto-aerodynamic flow past bodies*, Adv. in App. Mech. **8**, 1 (1964)
4. M. N. Kogan, *Magnetogasdynamics of plane and axisymmetric flows of a gas with infinite electrical conductivity*, Prikl. Mat. i Mekh. **23**, 70 (1959)
5. J. E. McCune and E. L. Resler, Jr., *Compressibility effects in magnetoaerodynamic flows past thin bodies*, Jr. of Aero/Space Sci. **27**, 493 (1960)
6. W. R. Sears, *On a boundary-layer phenomenon in magneto-fluid dynamics*, Astronautica Acta **7**, 223 (1961)
7. J. Y. T. Tang, M. Aero. E. Thesis, Cornell University, Ithaca, New York, 1966
8. D. N. Fan, *Aligned-fields magnetogasdynamic wakes*, Jr. of Fluid Mech. **20**, 433 (1964)